Intermittent reloading does not prevent iron availability decrease and hepcidin upregulation caused by hindlimb unloading

Kevin Nay, David J. R. Martin, Luz Orfila, Dany Saligaut, Brice Martin, Mathieu Horeau, Thibaut Cavey, Moussa Kenawi, Marie-Laure Island, Martine Ropert, et al.

Manuscript Submitted to Experimental Physiology

Intermittent reloading does not prevent iron availability decrease and hepcidin upregulation caused by hindlimb unloading

Kévin Nay[1,2], David Martin[1], Luz Orfila[1], Dany Saligaut[1], Brice Martin[1], Mathieu Horeau[1], Thibaut Cavey[3,4], Moussa Kenawi[3], Marie-Laure Island [3,4], Martine Ropert[3,4], Olivier Loréal[3], Christelle Koechlin-Ramonatxo[2], Frédéric Derbré[1].

[1]Laboratory "Movement Sport and Health Sciences" EA7470, University of Rennes/ENS Rennes, France
[2]DMEM, Univ Montpellier, INRA, Montpellier, France
[3]INSERM 1241, University of Rennes, Nutrition Metabolisms and Cancer (NuMeCan), Rennes, France
[4]Department of Biochemistry, CHU Rennes, France

Running head: Hindlimb unloading decreases iron availability

Keywords: disuse, physical inactivity, crosstalk, myosin heavy chain, iron overload

Corresponding author:

Frederic Derbré, PhD, Associate professor
Laboratory "Movement, Sport and Health Sciences" – EA7470
University of Rennes/ENS Rennes, 35170 Bruz, France
Mail: frederic.derbre@univ-rennes2.fr
Phone: (0033)290091587

ABSTRACT

In humans, exposure to microgravity during spaceflights causes muscle atrophy, iron storage changes, and iron availability reduction. We previously observed in rats that during simulated microgravity for 7 days, hepcidin plays a key role in iron misdistribution, and suggested that a crosstalk between skeletal muscle and liver could regulate hepcidin synthesis in this context. In the present study, we investigated in rats the medium-term effects of simulated microgravity on iron metabolism. We also tested whether intermittent reloading (IR) to target skeletal muscle atrophy efficiently limits iron misdistribution. To this purpose, Wistar rats underwent 14 days of hindlimb unloading (HU) combined or not with daily IR. At the end of this period, serum iron concentration and transferrin saturation were significantly reduced, whereas hepatic hepcidin mRNA was upregulated. However, the main signaling pathways involved in hepcidin synthesis in liver (BMP/SMAD, IL6/STAT3, and ERK1/2) were unaffected. Differently from what observed after 7 days of HU, iron concentration in spleen, liver and skeletal muscle was comparable between control and animals that underwent HU or HU+IR for 14 days. Despite its beneficial effect on soleus muscle atrophy and slow-to-fast myosin heavy chain distribution, IR did not significantly prevent iron availability reduction and hepcidin upregulation. Altogether, these results highlight that iron availability is durably reduced during longer exposure to simulated microgravity, and that the related hepcidin upregulation is not a transient adaptation to this condition. They also suggest that skeletal muscle does not necessarily play a key role in iron misdistribution occurring during simulated microgravity.

NEW FINDINGS

What is the central question of this study?

Could skeletal muscle be involved in microgravity-induced iron misdistribution by modulating hepcidin expression, the master regulator of iron metabolism?

What is the main finding and its importance?

We demonstrate in rats that hepcidin upregulation is not a transient adaptation associated with early exposure to microgravity, and that intermittent reloading does not limit microgravity-induced iron misdistribution despite a beneficial effect on soleus muscle wasting.

INTRODUCTION

During spaceflights, the astronauts' physical function is decreased, leading to reduced capacity to work, ability to carry out missions, and also complications during recovery. Lack of muscle activity due to microgravity considerably contributes to this functional decline through reduction of muscle mass and strength, impairment of cardiovascular performance, loss of bone mineral density, and also anemia (De Santo *et al.*, 2005; Pavy-Le Traon *et al.*, 2007; Pierre *et al.*, 2016). Astronauts and bedridden subjects also exhibit higher serum ferritin levels and lower serum iron and transferrin levels suggesting that microgravity increases iron store and reduces iron availability (Smith *et al.*, 2005; Morgan *et al.*, 2012; Zwart *et al.*, 2013). These iron metabolism alterations could play a key role in the appearance of anemia due to lower iron availability for erythropoiesis, but also in muscle atrophy and osteoporosis, because iron overload promotes oxidative stress in these organs through the Fenton reaction (Reardon & Allen, 2009; Tsay *et al.*, 2010).

Iron metabolism is mainly controlled by hepcidin, a 25 amino-acid peptide hormone that is secreted by liver and inhibits iron export through the degradation of the iron exporter ferroportin (Zhang, 2010). In addition, hepcidin reduces iron absorption by duodenal enterocytes. Consequently, hepcidin induces a decrease of blood iron availability and an increase of iron storage in cells that express ferroportin (i.e., macrophages and enterocytes). Although previous studies reported that serum ferritin levels are higher in astronauts and bedridden patients, indicative of increased iron storage (Smith *et al.*, 2005; Morgan *et al.*, 2012; Zwart *et al.*, 2013), the organs where iron accumulates remain unclear. Using the hindlimb unloading (HU) model to simulate microgravity in rats, we recently reported that

short-term exposure to microgravity (i.e., 7 days) decreases transferrin saturation and concomitantly increases iron concentration in spleen, but not in liver (Cavey *et al.*, 2017). These changes were associated with increased hepcidin synthesis in liver (Cavey *et al.*, 2017), suggesting that this hormone could play a key role in iron distribution alterations in conditions of microgravity.

Hepcidin is mainly upregulated in response to: 1) iron accumulation in the liver that activates the bone morphogenetic protein/SMAD (BMP/SMAD) signaling pathway; 2) inflammation that activates the interleukin-6/Janus kinase 2/signal transducer and activator of transcription 3 (IL-6/JAK2/STAT3) signaling pathway; 3) increase of transferrin-bound iron that activates ERK1/2 (Ramey *et al.*, 2009; Zhao *et al.*, 2013). In agreement, after 7 days of HU, we observed an increase of STAT3 activation in liver combined with *Il6* mRNA upregulation in atrophied rat skeletal muscle (Cavey *et al.*, 2017). Similarly to physical exercise known to upregulate hepcidin synthesis through an IL-6-dependent mechanism (Banzet *et al.*, 2012), these data suggest that microgravity early induces systemic pro-inflammatory state promoting hepcidin synthesis. They also raise questions about the transient or permanent nature of this physiological response to microgravity. As simulated microgravity increases IL-6 levels in atrophied muscle both in humans and rodents (Kang & Ji, 2013; Kwon *et al.*, 2015; Cavey *et al.*, 2017), these findings finally suggest that IL-6 could be involved in a muscle-to-liver crosstalk to regulate iron metabolism.

Intermittent muscle reloading (IR) during HU is considered an efficient strategy to limit muscle mass loss as well as reduction in fiber cross-sectional area (CSA) and muscle strength in rodents (Thomason *et al.*, 1987; Hauschka *et al.*, 1988; D'Aunno *et al.*, 1990, 1992; Bangart *et al.*, 1997). By modulating muscle plasticity, this experimental model constitutes an interesting tool to explore the role of skeletal muscle on iron metabolism regulation during simulated microgravity. Therefore, the aim of this study was to determine 1) whether medium-term HU affects iron distribution and hepcidin synthesis, and 2) whether IR (1h/day) could limit iron distribution alterations during HU by targeting skeletal muscle atrophy.

.

MATERIAL AND METHODS

Ethical approval

The experimental protocol and procedures used in this study were approved by the Rennes committee on Ethics in Research (authorization 8585-2017011709503125) and by the French Ministry of Higher Education.

Animals and experimental procedures

Male Wistar rats (7-week-old; Janvier Labs, Le Genest St Isle, France) were housed in a temperature-controlled room (21 ± 2°C) with a 12h:12h light/dark cycle and received standard rodent chow and water *ad libitum*. After 1 week of acclimatization, animals were randomly assigned to three experimental groups: non-suspended (control, n = 12), hindlimb unloading (HU, n = 12), and hind limb unloading with 1h reloading per day (HU-IR, n=12). HU was performed according to the Morey's tail suspension protocol (Morey-Holton & Globus, 2002). One 1h per day, HU-IR animals were removed from hindlimb suspension and free to perform ambulatory activity on their cage (i.e. 30cm x 30cm area). After 14 days, rats were deeply anaesthetized with a ketamine-xylazine-butorphanol cocktail. Liver, spleen, soleus and gastrocnemius were harvested, weighed, frozen in liquid nitrogen, or fixed in 4% paraformaldehyde (PFA). Intracardiac blood was collected in dry tubes. Hemoglobin concentration was determined using the HemoCue® 201+ system (HemoCue, AB, Meaux, France). Blood was then centrifuged (1 500 g, 10 min) for serum isolation. Rats were euthanized by exsanguination.

Biochemical methods

Serum iron and unsaturated iron binding capacity (UIBC) were measured using a Cobas 8000 analyzer (Roche®) with the Cobas® reagents 03183696 122 and 04536355 190, respectively (Roche Diagnostics, Meylan, France) at the biochemistry laboratory of Rennes Pontchaillou Hospital. Serum transferrin saturation was calculated as [serum iron/(serum iron + UIBC)] × 100 (Cavey *et al.*, 2015). Liver, spleen and gastrocnemius iron concentrations were quantified by inductively coupled plasma mass spectrometry, as previously described (Cavey *et al.*, 2015). Serum erythropoietin (EPO) and IL-6 concentrations were measured by ELISA, according to the manufacturer's instructions (BioLegend, London, UK).

.

Histological analyses

Soleus muscles were fixed in PFA and embedded in paraffin for 24 hours. Serial transverse sections of 4µm were cut from the wider part of each sample using a LEICA microtome, and were mounted on glass slides (3 sections/slide). Muscle sections were then stained using the Gomori's method to detect reticulin fibers. All stained sections were scanned (x20 objective) to measure the fiber CSA from at least 1000 fibers per muscle using the Image J software (NIH, Bethesda, MD).

Protein extraction

Protein extraction was performed from soleus muscle and liver in cold lysis buffer that contained 10.0mM Tris·HCl, pH 7.4, 0.5M sucrose, 50.0mM NaCl, 5.0mM EDTA, 30.0mM $Na_4P_2O_7$, 1% NP-40, 0.25% sodium deoxycholate, 50.0mM NaF, 100.0µM sodium orthovanadate, and protease inhibitor cocktail (5µl/ml, P8340; Sigma, St. Louis, MO). Samples were homogenized using a Polytron homogenizer at 4°C. Each sample was then incubated on ice for 30 min followed by sonication (3x10s). Homogenates were transferred to microcentrifuge tubes and centrifuged at 12,000g at 4°C for 12 min. Protein concentration in supernatants was determined with the Lowry assay using BSA as standard. Samples were then diluted in SDS-PAGE sample buffer (50mM Tris·HCl, pH 6.8, 2% SDS, 10% glycerol, 5% β-mercaptoethanol, and 0.1% bromophenol blue) and heated at 95°C for 5 min.

Western blotting

Samples containing 50-100µg of proteins were resolved on 12.5% SDS-PAGE. Proteins were transferred onto a 0.2µm nitrocellulose membrane at 240 mA for 90 min. Membranes were blocked with 5% BSA or nonfat dry milk in Tris-buffered saline/0.05% Tween-20 (TBST) at room temperature for 1 hour. Membranes were incubated at 4°C with the appropriate primary antibodies (Table 1) overnight. Then, membranes were washed with TBST and incubated at room temperature with infrared dye-conjugated secondary antibodies (LI-COR, Lincoln, NE) for 1 hour. After washing, blots were imaged with the Odyssey Imaging System (LI-COR). All blots were scanned, and densitometric analysis was performed using a GS-800 Calibrated Imaging Densitometer and the Quantity One software. The phosphorylation-specific signal was normalized to the total signal to estimate the ratio of activated marker.

Myosin heavy chain isoform distribution

The muscle fiber phenotype was determined by assessing the presence of the different myosin heavy chain (MHC) isoforms (slow MHC I and fast MHC IIa, IId/x, IIb isoforms), as

.

previously described (Talmadge & Roy, 1993; Nay *et al.*, 2019). Protein samples (6 µg) were separated on high-glycerol-containing (30%) gels with an acrylamide-to-bis-acrylamide ratio of 50:1 for the separating gel (8% total acrylamide, pH 8.8) and for the stacking gel (4% total acrylamide, pH 6.8) using a Mini-Protean II dual slab cell apparatus (Bio-Rad, Hercules, CA). After electrophoresis (at 140V in a refrigerated room at 4°C for 22h), gels were stained with Coomassie blue (IRDye® Blue Protein Stain, LI-COR Biosciences, Lincoln, NE, USA) and the different MHC isoforms were identified according to their electrophoretic mobility pattern (Derbré *et al.*, 2016; Nay *et al.*, 2019).

RNA extraction and quantitative real-time PCR

Total RNA was extracted from liver (~30 mg) and soleus (~15 mg) with TRIzol® (Invitrogen, Vilvoorde, Belgium), according to the manufacturer's instructions. RNA quality and quantity were assessed by 1.5% agarose gel electrophoresis and Nanodrop® spectrophotometry. Reverse transcription was performed with the iScript cDNA Synthesis Kit (Bio-Rad) using 1 µg total RNA. Real-time PCR experiments were done on a MyIQ2 thermocycler (Bio-Rad) using the following conditions: 3 min at 95°C, followed by 35 cycles of 30 s at 95°C, 30 s at 60°C and 30 s at 72°C. Samples were analyzed in duplicate in 10 µl reaction volume containing 4.8 µl IQSybrGreen SuperMix (Bio-Rad), 0.1 µl of each primer (100nM final), and 5 µl cDNA. Primer sequences are in Table 2. Melting curves were systematically analyzed to ensure the amplification specificity. The expression level of the target genes was normalized using three reference genes according to geNorm (Vandesompele *et al.*, 2002), and expressed relative to the control group. The references genes were ribosomal protein L4 (*Rpl4*), glyceraldehyde-3-phosphate dehydrogenase (*Gapdh*), and hypoxanthine phosphoribosyltransferase 1 (*Hprt1*).

Statistical analysis

All data are presented as the mean ± standard error of the mean (SEM). The normality of each distribution and homogeneity of variance were assessed with the Kolmogorov-Smirnov and Bartlett test, respectively. A one-way analysis of variance (ANOVA) was then performed. Significant interaction effects were analyzed with the Fisher's Least Significant Difference (LSD) post-hoc test. The Kruskal Wallis test was chosen when the normality and/or equal variance test failed. For all statistical analyses, the significance level was set at 0.05. Data were analyzed using the statistical package GraphPad Prism version 6.02 for Windows (GraphPad Software, La Jolla, California).

.

RESULTS

Intermittent reloading prevents HU-induced soleus atrophy. Body weight and the muscle weight-to-body weight ratio are shown in Table 3. After 14 days of HU, soleus and gastrocnemius weight-to body weight ratio were reduced by 46% and 19%, respectively in the HU group compared with control rats ($p<0.001$, Table 3). The soleus muscle mass reduction was associated with a lower mean fiber CSA in the HU than control group (-62%, $p<0.001$, Fig. 1A and B). IR (HU-IR group) attenuates the reduction of soleus muscle mass and fiber CSA compared with HU alone (HU group) (+36%, $p<0.001$ and +58%, $p<0.001$ respectively) (Table 3 and Fig. 1A and B). Conversely, gastrocnemius weight-to body weight ratio was comparable in HU and HU-IR rats (Table 3).

Microgravity-induced muscle atrophy is associated with imbalance between muscle protein synthesis and breakdown (Chopard *et al.*, 2009). These alterations of protein turnover are generally characterized by inhibition of the anabolic AKT/mammalian target of rapamycin (mTOR) signaling pathways and increased activity of the catabolic ubiquitin-proteasome pathway (Chopard *et al.*, 2009). In agreement, western blot analysis and quantification of the relative phosphorylation levels of key markers of these signaling pathways showed that activation of AKT was decreased whereas that of 4E-BP1 (mTOR target) was increased in soleus protein lysates from HU rats compared with controls (-28%, $p=0.054$ and +29%, $p<0.001$, respectively, Fig. 1C-D). This was associated with higher protein ubiquitination levels after HU (+21% compared with controls, $p=0.012$, Fig. 1C-D). IR prevented HU effect on AKT activation and protein ubiquitination (values comparable in HU-IR animals and controls) (Fig 1C-D), but not on 4E-PB1 phosphorylation (+15% compared with controls, $p<0.001$, Fig. 1C-D).

Intermittent reloading prevents the slow-to-fast MHC phenotype transition in soleus muscle. Analysis of the relative contents of the fast and slow MHC isoforms in the three experimental groups (representative SDS-PAGE in Fig. 1E) showed that expression of type I slow MHC (MHC I), the predominant form in control soleus muscles (90%), was significantly reduced in the HU group (76%, $p=0.002$, Fig. 1E and F). Conversely, MHC IIx (from 1 to 7%, $p<0.001$) and MHC IIb (from 1 to 6%, $p<0.001$) (Fig. 1E and F) significantly increased. MHC IIa did not significantly differ between control and HU animals ($p=0.32$, Fig. 1E and F). MHC I expression was similarly decreased in the HU-IR group compared with controls (90 vs. 78%, $p=0.004$, Fig. 1E and F), whereas only MHC IIa was significantly increased in these animals

.

(from 7 to 17%, p=0.003, Fig. 1E and F). IR efficiently attenuated the MHC IIx and MHC IIb increase observed in the HU group (7% versus 2%, p<0.001 and 6% versus 2% in the HU and HU-IR group, respectively; p<0.001 for both, Fig. 1E and F).

Effects of 14 days of hindlimb unloading and intermittent reloading on iron distribution. We then determined the iron metabolism changes induced by HU, and whether they can be influenced by IR. After 14 days of HU, serum iron concentration (-21%, p=0.019, Table. 4) and transferrin saturation (-18%, p=0.041, Table. 4) were significantly reduced in the HU group compared with controls. This reduction of the available iron was not associated with changes in hemoglobin, hematocrit, and serum EPO levels (Table 4). To determine where iron was stored during HU, we measured iron concentration in liver and spleen, the main organs responsible for iron storage. We found no difference between control and HU rats in liver and spleen iron content. As muscle atrophy could affect iron metabolism, we also measured iron concentration in gastrocnemius muscles, but did not find any difference between control and HU rats. Despite the positive effect on soleus muscle atrophy, HU+IR group failed to significantly prevent decreases of serum iron concentration and transferrin saturation observed in HU group (Table. 4). Furthermore, serum iron concentration, liver, spleen and skeletal muscle iron concentrations, as well as hemoglobin, hematocrit and serum EPO levels were not altered in HU+IR group vs CTL and HU groups (Table. 4).

Effects of 14 days of hindlimb unloading and intermittent reloading on hepcidin regulation. To investigate the mechanism by which HU affected iron availability, we quantified the liver expression of hepcidin, the master regulator of iron metabolism. Hepcidin mRNA level (*Hamp*) was increased in the HU group compared with control (+77%, p=0.036, Fig. 2A), suggesting a role for this hormone in the iron homeostasis alteration during HU. In agreement with the lack of preventive effects of HU-IR on iron availability reduction, *Hamp* level was also increased in the HU-IR group compared with control (+95%, p=0.008, Fig. 2A). Hepcidin expression is upregulated by different signaling pathways, including BMP6/SMAD, ERK1/2 and IL-6/STAT3 (52). Therefore, we investigated whether these three signaling pathways were activated in the liver of HU and HU-IR animals. However, we did not detect any change in STAT3, SMAD1-5-8 and ERK activation (Fig. 2B-C). Furthermore, mRNA expression of C-reactive protein (*Crp*) and haptoglobin (*Hp*) in liver was not significantly different in the three groups.

.

DISCUSSION

The present study was designed to evaluate the medium-term effect of simulated microgravity on iron metabolism, and to determine the role of skeletal muscle in iron metabolism regulation in this specific condition. Using a HU rat model, we previously demonstrated that 7 days of exposure leads to hepcidin upregulation and concomitantly to iron distribution changes (Cavey *et al.*, 2017). In the present study, we found that iron availability remains low after 14 days of HU, probably due to persistent hepcidin upregulation. Moreover, we observed that IR efficiently prevents HU-induced soleus atrophy and slow-to fast twitch MHC isoform transition. However, it cannot prevent the reduction of iron availability and hepcidin upregulation.

During space missions, microgravity reduces serum iron concentration and increases iron storage in humans (Smith *et al.*, 2005). The HU model has been widely used for decades to mimic the effects of microgravity on the organism during spaceflight. This model presents the advantage of exploring the organ-specific responses to microgravity, a key characteristic of the spaceflight environment, but without the concomitant effects of the exposure to radiation or hypercapnia. In a previous study, we found that 7 days of HU reduces circulating iron concentration and transferrin saturation in rats (Cavey *et al.*, 2017). Here, we obtained similar results after 14 days of HU, suggesting that the available iron is reduced also upon prolonged exposure to simulated microgravity. The decreased iron availability for erythropoiesis could play an important role in spaceflight anemia (Smith, 2002). In our previous study, we found that 7 days of HU reduces also serum EPO concentrations in rats (unpublished data), as reported in humans after short-term exposure to real and simulated microgravity (Leach *et al.*, 1988; Gunga *et al.*, 1996). Conversely, here we found that serum EPO concentrations did not differ between controls and rats exposed to HU for 14 days. This suggests that erythropoiesis decrease might play a role in anemia only during the first days of exposure to microgravity.

To understand whether iron metabolism is dysregulated in conditions of simulated microgravity, we investigated hepcidin synthesis in the liver of HU rats. We found that hepcidin transcription was increased after 14 days of HU in the same order of magnitude we previously observed after 7 days of HU (Cavey *et al.*, 2017). High hepcidin levels induce the decrease of serum iron concentration and the increase of iron storage in cells that express ferroportin, especially macrophages (Ganz, 2011). After 7 days of HU, we previously

.

observed that iron accumulates in spleen, which is particularly rich in macrophages (Cavey *et al.*, 2017), but not in liver. Here, we found that iron concentrations in spleen and liver were not significantly different in HU rats (14 days) and controls. On the other hand, Xu *et al*. reported that 21 days of HU increases iron concentration in liver (Xu *et al.*, 2017). These results suggest that splenic iron storage during the first days of HU is transient, possibly to protect other organs from iron overload. However, this mechanism might not be effective when exposure to mechanical unloading is prolonged. The fact that serum iron concentration (and thus availability) remained low after 14 days of HU, despite the return to normal iron concentration in spleen, suggests that iron started to accumulate in other organs. Therefore, we also measured iron concentration in atrophied gastrocnemius muscles, but levels were comparable in controls and rats that experienced HU for 14 days. It would be interesting to explore the effects of prolonged real and simulated microgravity on iron storage in other organs that are functionally affected by this condition (e.g., brain, kidney, heart).

We previously showed that in rats, HU for 7 days increases STAT3 activation in liver (Cavey *et al.*, 2017). Conversely, after 14 days of HU, activation of STAT3 and of the BMP/SMAD and ERK1/2 signaling pathways was comparable in control and HU rats. Recently, Xu et al (2017) observed in mice that after 21 days of HU, *Bmp6* mRNA levels are increased and hepcidin upregulated. Altogether, these data support the hypothesis that hepcidin upregulation is not a transient adaptation associated with mechanical unloading, and that the underlying mechanisms differ depending on the exposure duration. Thus, low-grade inflammation might play a role during the first days of simulated microgravity; however, upon prolonged exposure other mechanisms might be involved, including iron overload in liver.

In our previous study we observed that 7 days of HU also increases *Il6* mRNA levels in atrophied skeletal muscle, concomitantly with STAT3 activation in liver (Cavey *et al.*, 2017). Therefore, we proposed the existence of a muscle-to-liver crosstalk to regulate iron metabolism under microgravity. As mechanical unloading increases both circulating and muscle IL-6 levels in humans and rodents (Felix *et al.*, 2004; Bosutti *et al.*, 2008; Mutin-Carnino *et al.*, 2014; Kwon *et al.*, 2015; Cavey *et al.*, 2017; Yakabe *et al.*, 2018), we hypothesized that IR would prevent hepcidin upregulation and the related iron distribution changes by limiting muscle atrophy and the associated inflammatory state. Here, we did not find any preventive effect of IR on iron metabolism, although it limited HU-induced soleus

.

muscle atrophy and the transition from the slow to fast muscle contractile phenotype. These results refute the hypothesis of a skeletal muscle-liver dialogue during mechanical unloading. However, IR prevented HU-induced atrophy of the soleus muscle, but less efficiently the atrophy of the gastrocnemius muscle. In rats, this muscle represents a mass approximately 20 times bigger than that of the soleus muscle. Based on this data, we cannot exclude that the IR preventive effect on whole-body skeletal muscle mass was too small to significantly influence iron metabolism regulation. Moreover, after 14 days of HU, the IL-6/STAT3 signaling pathway was no longer activated in liver, both in the HU and HU-IR groups. Therefore, we cannot exclude that IR might exert a preventive effect on hepcidin synthesis during the first days of mechanical unloading that are characterized by an intense catabolic and inflammatory state of skeletal muscle. This effect might then decrease after 14 days, following the progressive reduction of the systemic and muscle inflammatory state.

To conclude, the present study demonstrates in rats that iron availability is durably reduced during simulated microgravity, but that iron distribution changes differ after short and medium-term exposure to HU. It also confirms that hepcidin plays a key role in this process, although the underlying mechanisms are still unclear. Finally, IR effectively prevented HU-induced soleus wasting, but did not have any effect on iron distribution changes, suggesting that skeletal muscle might not be a key player in iron balance regulation in conditions of microgravity.

ACKNOWLEDGMENTS

The authors thank Pascale Bellaud (H2P2 facility, University Rennes 1, Rennes) for technical help with histological analyses, and Guillemette Gauquelin-Koch (Centre National d'Etudes Spatiales, Paris) for scientific support. The authors thank Elisabetta Andermarcher for expert manuscript editing.

AUTHOR CONTRIBUTIONS

F.D. and O.L. designed the study. K.N., D.M., L.O., D.S., B.M., M.H., T.C., M.K., M.-L.I., M.R., O.L., C.K.-R. and F.D. performed experiments, analyzed data and interpreted results. K.N., D.M., L.O., D.S., B.M., M.H., T.C., M.K., M.-L.I., M.R., O.L., C.K.-R. and F.D. drafted manuscript and figures or revised them critically for important intellectual content. All authors approved the final version of the manuscript and agree to be accountable for all aspects of the work in ensuring that questions related to the accuracy or integrity of any part

.

of the work are appropriately investigated and resolved. All persons designated as authors qualify for authorship, and all those who qualify for authorship are listed.

GRANTS

This study was supported by grants from the French "Centre National d'Etudes Spatiales" (CNES), the Brittany Research Council, and INRA.

DISCLOSURES

No conflict of interest, financial or otherwise, is declared by the author(s).

REFERENCES

Bangart JJ, Widrick JJ & Fitts RH (1997). Effect of intermittent weight bearing on soleus fiber force-velocity-power and force-pCa relationships. *J Appl Physiol* **82,** 1905–1910.

Banzet S, Sanchez H, Chapot R, Bigard X, Vaulont S & Koulmann N (2012). Interleukin-6 contributes to hepcidin mRNA increase in response to exercise. *Cytokine* **58,** 158–161.

Bosutti A, Malaponte G, Zanetti M, Castellino P, Heer M, Guarnieri G & Biolo G (2008). Calorie restriction modulates inactivity-induced changes in the inflammatory markers C-reactive protein and pentraxin-3. *J Clin Endocrinol Metab* **93,** 3226–3229.

Cavey T, Pierre N, Nay K, Allain C, Ropert M, Loréal O & Derbré F (2017). Simulated microgravity decreases circulating iron in rats: role of inflammation-induced hepcidin upregulation. *Exp Physiol* **102,** 291–298.

Cavey T, Ropert M, de Tayrac M, Bardou-Jacquet E, Island M-L, Leroyer P, Bendavid C, Brissot P & Loréal O (2015). Mouse genetic background impacts both on iron and non-iron metals parameters and on their relationships. *Biometals* **28,** 733–743.

Chopard A, Hillock S & Jasmin BJ (2009). Molecular events and signalling pathways involved in skeletal muscle disuse-induced atrophy and the impact of countermeasures. *J Cell Mol Med* **13,** 3032–3050.

D'Aunno DS, Robinson RR, Smith GS, Thomason DB & Booth FW (1992). Intermittent acceleration as a countermeasure to soleus muscle atrophy. *J Appl Physiol* **72,** 428–433.

D'Aunno DS, Thomason DB & Booth FW (1990). Centrifugal intensity and duration as countermeasures to soleus muscle atrophy. *J Appl Physiol* **69,** 1387–1389.

De Santo NG, Cirillo M, Kirsch KA, Correale G, Drummer C, Frassl W, Perna AF, Di Stazio E, Bellini L & Gunga H-C (2005). Anemia and erythropoietin in space flights. *Semin Nephrol* **25,** 379–387.

.

Derbré F, Droguet M, Léon K, Troadec S, Pennec J-P, Giroux-Metges M-A & Rannou F (2016). Single Muscle Immobilization Decreases Single-Fibre Myosin Heavy Chain Polymorphism: Possible Involvement of p38 and JNK MAP Kinases. *PLoS ONE* **11,** e0158630.

Felix K, Wise K, Manna S, Yamauchi K, Wilson BL, Thomas RL, Kulkarni A, Pellis NR & Ramesh GT (2004). Altered cytokine expression in tissues of mice subjected to simulated microgravity. *Mol Cell Biochem* **266,** 79–85.

Ganz T (2011). Hepcidin and iron regulation, 10 years later. *Blood* **117,** 4425–4433.

Gunga HC, Kirsch K, Baartz F, Maillet A, Gharib C, Nalishiti W, Rich I & Röcker L (1996). Erythropoietin under real and simulated microgravity conditions in humans. *J Appl Physiol* **81,** 761–773.

Hauschka EO, Roy RR & Edgerton VR (1988). Periodic weight support effects on rat soleus fibers after hindlimb suspension. *J Appl Physiol* **65,** 1231–1237.

Kang C & Ji LL (2013). Muscle immobilization and remobilization downregulates PGC-1α signaling and the mitochondrial biogenesis pathway. *J Appl Physiol* **115,** 1618–1625.

Kwon OS, Tanner RE, Barrows KM, Runtsch M, Symons JD, Jalili T, Bikman BT, McClain DA, O'Connell RM & Drummond MJ (2015). MyD88 regulates physical inactivity-induced skeletal muscle inflammation, ceramide biosynthesis signaling, and glucose intolerance. *Am J Physiol Endocrinol Metab* **309,** E11-21.

Leach CS, Johnson PC & Cintrón NM (1988). The endocrine system in space flight. *Acta Astronaut* **17,** 161–166.

Morey-Holton ER & Globus RK (2002). Hindlimb unloading rodent model: technical aspects. *J Appl Physiol* **92,** 1367–1377.

Morgan JLL, Zwart SR, Heer M, Ploutz-Snyder R, Ericson K & Smith SM (2012). Bone metabolism and nutritional status during 30-day head-down-tilt bed rest. *J Appl Physiol* **113,** 1519–1529.

Mutin-Carnino M, Carnino A, Roffino S & Chopard A (2014). Effect of muscle unloading, reloading and exercise on inflammation during a head-down bed rest. *Int J Sports Med* **35,** 28–34.

Nay K, Jollet M, Goustard B, Baati N, Vernus B, Pontones M, Lefeuvre-Orfila L, Bendavid C, Rué O, Mariadassou M, Bonnieu A, Ollendorf V, Lepage P, Derbré F & Koechlin-Ramonatxo C (2019). Gut bacteria are critical for optimal muscle function: a potential link with glucose homeostasis. *Am J Physiol End Meta*.

Pavy-Le Traon A, Heer M, Narici MV, Rittweger J & Vernikos J (2007). From space to Earth: advances in human physiology from 20 years of bed rest studies (1986-2006). *Eur J Appl Physiol* **101,** 143–194.

.

Pierre N, Appriou Z, Gratas-Delamarche A & Derbré F (2016). From physical inactivity to immobilization: Dissecting the role of oxidative stress in skeletal muscle insulin resistance and atrophy. *Free Radic Biol Med* **98,** 197–207.

Ramey G, Deschemin J-C & Vaulont S (2009). Cross-talk between the mitogen activated protein kinase and bone morphogenetic protein/hemojuvelin pathways is required for the induction of hepcidin by holotransferrin in primary mouse hepatocytes. *Haematologica* **94,** 765–772.

Reardon TF & Allen DG (2009). Iron injections in mice increase skeletal muscle iron content, induce oxidative stress and reduce exercise performance. *Exp Physiol* **94,** 720–730.

Smith SM (2002). Red blood cell and iron metabolism during space flight. *Nutrition* **18,** 864–866.

Smith SM, Zwart SR, Block G, Rice BL & Davis-Street JE (2005). The nutritional status of astronauts is altered after long-term space flight aboard the International Space Station. *J Nutr* **135,** 437–443.

Talmadge RJ & Roy RR (1993). Electrophoretic separation of rat skeletal muscle myosin heavy-chain isoforms. *J Appl Physiol* **75,** 2337–2340.

Thomason DB, Herrick RE & Baldwin KM (1987). Activity influences on soleus muscle myosin during rodent hindlimb suspension. *J Appl Physiol* **63,** 138–144.

Tsay J, Yang Z, Ross FP, Cunningham-Rundles S, Lin H, Coleman R, Mayer-Kuckuk P, Doty SB, Grady RW, Giardina PJ, Boskey AL & Vogiatzi MG (2010). Bone loss caused by iron overload in a murine model: importance of oxidative stress. *Blood* **116,** 2582–2589.

Vandesompele J, De Preter K, Pattyn F, Poppe B, Van Roy N, De Paepe A & Speleman F (2002). Accurate normalization of real-time quantitative RT-PCR data by geometric averaging of multiple internal control genes. *Genome Biol* **3,** RESEARCH0034.

Xu Z, Sun W, Li Y, Ling S, Zhao C, Zhong G, Zhao D, Song J, Song H, Li J, You L, Nie G, Chang Y & Li Y (2017). The regulation of iron metabolism by hepcidin contributes to unloading-induced bone loss. *Bone* **94,** 152–161.

Yakabe M, Ogawa S, Ota H, Iijima K, Eto M, Ouchi Y & Akishita M (2018). Inhibition of interleukin-6 decreases atrogene expression and ameliorates tail suspension-induced skeletal muscle atrophy. *PLoS One*; DOI: 10.1371/journal.pone.0191318.

Zhang A-S (2010). Control of Systemic Iron Homeostasis by the Hemojuvelin-Hepcidin Axis12. *Adv Nutr* **1,** 38–45.

Zhao N, Zhang A-S & Enns CA (2013). Iron regulation by hepcidin. *J Clin Invest* **123,** 2337–2343.

.

Zwart SR, Morgan JLL & Smith SM (2013). Iron status and its relations with oxidative damage and bone loss during long-duration space flight on the International Space Station. *Am J Clin Nutr* **98,** 217–223.

TABLES

Table 1: List of primary antibodies used for western blotting

Antibody target	Molecular weight (kDa)	Reference	Dilution
Phosphorylated 4E-BP1$^{Thr37/46}$	15 to 20	Cell Signaling, 2855	1:1000
4E-BP1	15 to 20	Cell Signaling, 9644	1:1000
Phosphorylated AKT^{Ser473}	60	Cell Signaling, 9271	1:1000
AKT	60	Cell Signaling, 9272	1:1000
Phosphorylated ERK1/2$^{Thr202/Tyr204}$	42/44	Cell Signaling, 9101	1:1000
ERK1/2	42/44	Santa Cruz, sc-514302	1:200
HSC70	70	Cell Signaling, 9271	1:5000
Phosphorylated SMAD1/5/8$^{Ser463/465}$	60	Abcam, ab92698	1:1000
SMAD5	60	Cell Signaling, 12534	1:1000
Phosphorylated STAT3^{Tyr705}	90	Cell Signaling, 9131	1:1000
STAT3	86	Cell Signaling, 4904	1:1000
Ubiquitin		Cell Signaling, 3933	1:1000

.

Table 2. Primer sequences (5'–3')

Gene	Reference	Forward	Reverse
Crp	NM_017096.3	AGGCTTTTGGTCATGAAGACATG	CTTCGGCTCACATCAGCGT
Gapdh	NM_017008.4	GGTCGGTGTGAACGGATTTG	CGTGGGTAGAGTCATACTGGAACA
Hp	NM_012582.2	AACACTTGGTTCGTTATCGCTG	CCACACACTGCCTCACACTTG
Hamp	NM_053469.1	CTGCAGCCTTGGCATGG	CAGCAGCGCA CTGTCATCA -3
Hprt1	XM_008773659.2	CTGATTATGGACAGGACTGAAAGAC	CCAGCAGGTCAGCAAAGAACT
Rpl4	NM_022510.1	CGAGCACCACGCAAGAAGAT	ATTCCTAGCCTGGCGGAGAA

.

Table 3. Effect of hind limb unloading (HU) and intermittent reloading (IR) on body and organ weights. Values are the mean ± SD. Significant differences (P <0.05) are indicated as follows: [a]: comparison *versus* control group, [b]: comparison between HU and HU-IR. (n=9-12 for each group).

	Control	HU	HU-IR
Body weight (g)	413.9±31.2	336.3±25.4[a]	351.1±24.9[a]
Soleus weight (mg)	182.1±14.3	81.0±9.8[a]	115.5±14.9[a,b]
Soleus weight-to-body weight ratio (mg/100 g)	44.0±2.2	24.2 ±3.2[a]	33.0±4.8[a,b]
Gastrocnemius weight (mg)	2247.0±139.4	1490.3±124.2[a]	1678.2±134.0[a,b]
Gastrocnemius weight-to-body weight ratio (mg/100 g)	544.3±36.3	444.9±43.1[a]	479.8±48.8[a]
Liver weight (g)	13.9±1.9	10.8 ±1.5[a]	11.0±1.7[a]
Liver weight-to- body weight ratio (g/100 g)	3.4±0.4	3.2±0.4	3.2±0.5
Spleen weight (mg)	1044.0±153.1	937.0±137.8	964.9±132.2
Spleen weight-to-body weight ratio (mg/100 g)	251.5±25.2	278.0±32.0	275.3±36.0

.

Table 4. Effect of hind limb unloading (HU) and intermittent reloading (IR) on iron distribution and hematological parameters. Values are the mean ± SD. Differences were assessed by one-way ANOVA followed by the Fisher's LSD post-hoc test, and indicated as follows: [a]: comparison *versus* control group ($p<0.05$), (n=9-12 for each group).

	Control	HU	HU-IR
Iron metabolism			
Serum iron concentration (µmol/L)	35.7±7.5	28.2±4.4[a]	33.9±8.5
Transferrin saturation (%)	45.2±8.5	38.1±5.8[a]	39.3±8.4
Liver iron content (µg/g)	348.7±85.3	344.7±121.1	327.8±85.5
Spleen iron content (µg/g)	1578±456	1808±380	1523±471
Gastrocnemius iron content (µg/g)	53.8±10.2	56.6±4.6	59.2±16.8
Hematology			
Hematocrit (%)	47.5±2.9	48.5±2.0	48.0±1.7
Hemoglobin (g/dL)	17.4±1.5	17.5±0.6	17.4±0.6
EPO (mU/mL)	2.9±1.0	3.2±1.1	3.0±0.7

.

Figure 1: Effect of hindlimb unloading and intermittent reloading on soleus mass and contractile phenotype. (A) Representative cross-sectional area images in soleus, (B) Quantification (mean ± SD) of soleus cross-sectional area (µm²), (C) Representative blot of phosphorylated AKT on Ser473, AKT, phosphorylated 4E-BP1 on Thr37/46, 4E-BP1 and ubiquitinated proteins. HSC70 was used as loading control, (D) AKT and 4E-BP1 activation (phosphorylated/total protein ratio) and ubiquitin profile in soleus muscle (mean ± SD), (E) Representative electrophoresis of soleus myosin heavy chain (MHC) isoforms, (F) Distribution of MHC isoforms in soleus muscle (mean ± SD). Differences were assessed by a one-way ANOVA followed by the Fisher's LSD post-hoc test and indicated as follows: a: comparison *versus* control group ($p<0.05$), b: comparison between HU and HU-IR groups ($p<0.05$) (n=8-9 for each group); *: p=0.054 between control and HU rats.

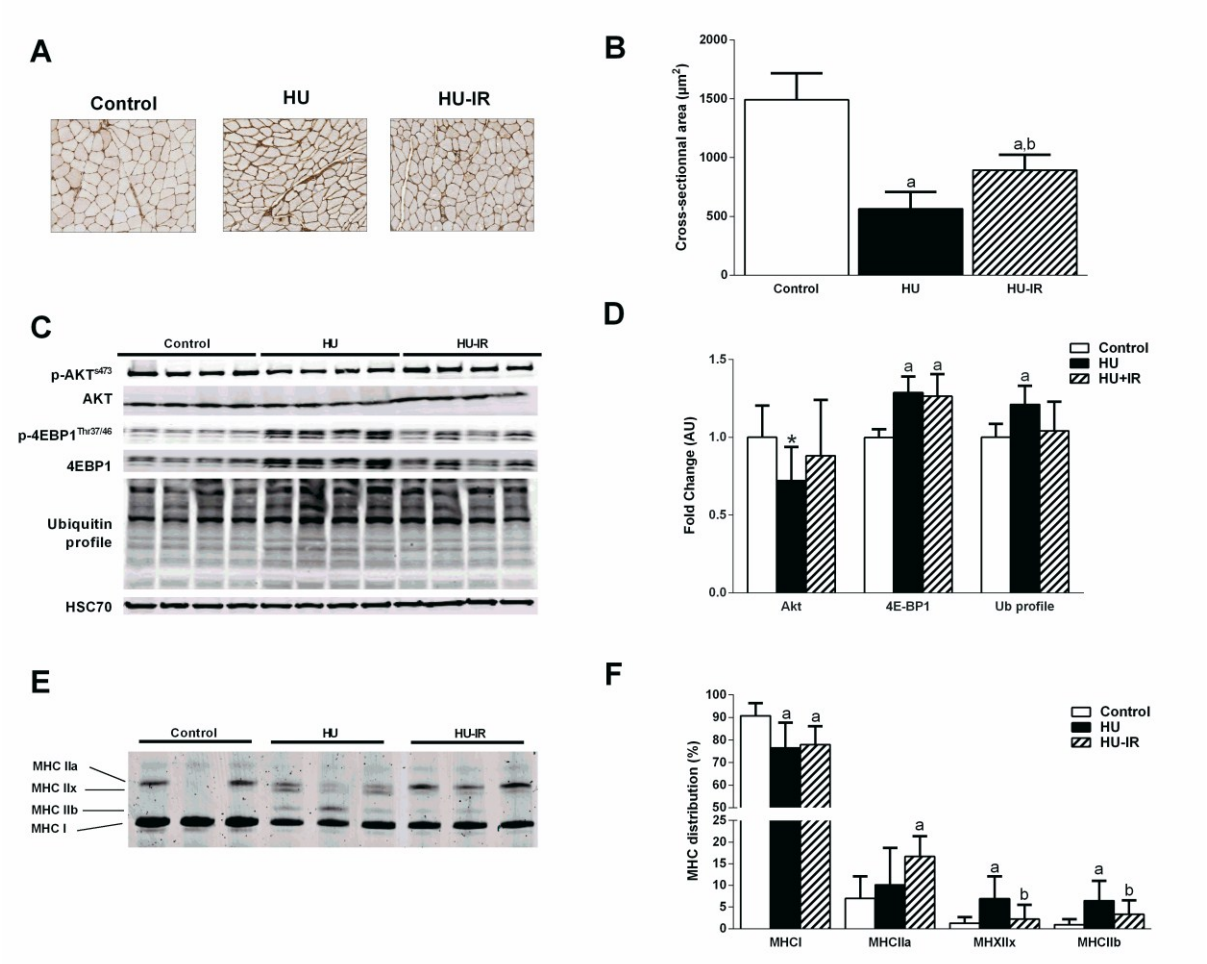

.

Figure 2: Effect of hindlimb unloading and intermittent reloading on liver hepcidin regulation. (A) Liver hepcidin, C-reactive protein and haptoglobin mRNA levels (mean ± SD), (B) Quantification (phosphorylated/total protein ratio) of STAT3, SMAD1/5/8, and ERK1-2 activation in liver (mean ± SD), (C) Representative blots of phosphorylated and total proteins involved in hepcidin regulation. Differences were assessed by one-way ANOVA followed by the Fisher's LSD post-hoc test, and indicated as follows: a: comparison *versus* control group ($p < 0.05$), b: comparison between HU and HU-IR groups ($p < 0.05$) (n=7-9 for each group).

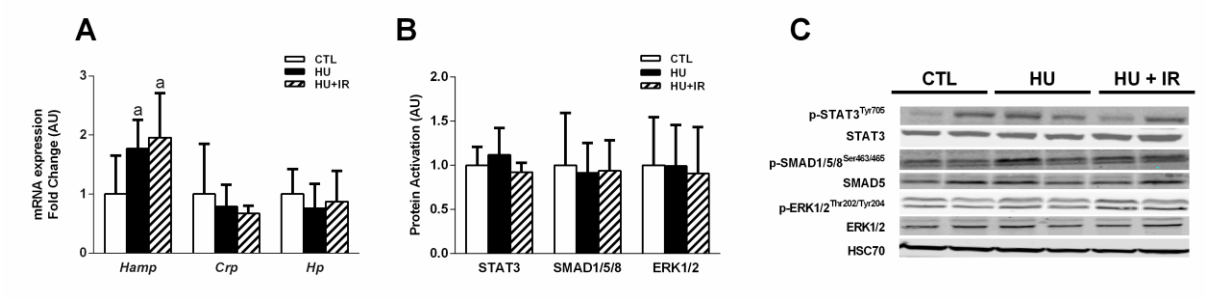

.